Polymer Degradation and Stability 191 (2021) 109655

Contents lists available at ScienceDirect

Polymer Degradation and Stability

journal homepage: www.elsevier.com/locate/polymdegradstab

Microfibrous cyclodextrin boosts flame retardancy of poly(lactic acid)

Kata Decsov, Viktor Takács, György Marosi, Katalin Bocz*

Budapest University of Technology and Economics, Department of Organic Chemistry and Technology, Budafoki street 8, H-1111, Budapest, Hungary

ARTICLE INFO

Article history:
Received 14 April 2021
Revised 7 June 2021
Accepted 13 June 2021
Available online 19 June 2021

Keywords:
Poly(lactic acid)
Intumescent flame retardant
Cyclodextrin
Microfibre
Electrospinning

ABSTRACT

2-hydroxypropyl-β-cyclodextrin (HP-β-CD) microfibres with diameters ranging between 3 and 7 μm were prepared by aqueous solution based high-speed electrospinning (HSES) technique and then used as carbonising agent at 3 wt% loading besides 15 wt% ammonium polyphosphate (APP) to obtain flame-retarded poly(lactic acid) (PLA) composites. The high specific surface area of the microfibrous HP-β-CD was found to have a crucial role in its flame retardant efficiency. Compared to the effect of the same amount of conventional HP-β-CD powder additive, microfibrous HP-β-CD resulted in higher char yields both during thermogravimetric analysis and cone calorimeter test accompanied with significantly increased mechanical resistance and consequently with improved flame retarding efficacy. The Limiting Oxygen Index (LOI) of the intumescent flame-retarded PLA composite increased noticeably, from 29.0% to 32.5%, while the Flame Retardancy Index (FRI), determined from cone calorimetry data, increased from 1.9 (with powder HP-β-CD) to 2.6 (with microfibrous HP-β-CD) only by changing the physical form i.e. the specific surface area of the used HP-β-CD. The advantage of the special microfibrous structure of the oligosaccharide type charring agent lies in the efficient interaction with APP and the attribution of the intumescent char layer with improved thermal and mechanical resistance without compromising its swelling ability. Besides, the microfibrous structure of the HP-β-CD also contributed to the improvement of the mechanical performance of the flame retarded PLA composites.

1. Introduction

The growing concern over the environment and sustainability lead to extensive research in developing bio-based green materials as means of solving the disposal problem and reducing the environmental impact of conventional plastics [1]. Among biodegradable thermoplastics, poly(lactic acid) (PLA) (derived from starches and sugars [2]) has received increasing attention from industry and academia [3,4] because of its biodegradability, excellent mechanical properties, thermoplastic processability, and biological properties. Because of these properties, PLA is proving to be useful in diverse applications as a viable alternative to petrochemical-based plastics [4]. PLA's applications have extended from short life cycle products to the electronics, automobiles, building materials, and the aerospace industry [5–8]. Since without flame retardants (FRs) PLA cannot meet the safety standards in most cases, the development of effective flame retardants for the modification of PLA is necessitated [9,10]. Intumescent flame-retardant systems (IFRs) are considered promising halogen-free flame-retardant additives that form a foamed cellular charred layer on the surface of the polymer matrix to block the combustion process resulting in lower smoke emission and toxicity and suppressed molten dripping during a fire [11]. These systems mainly include three components; a carbonization agent, an acid source, and a blowing agent [12]. Ammonium polyphosphate (APP) can act both as the acid source and the blowing agent often combined with a polyalcohol type carbonization agent like pentaerythritol (PER) [13]. The use of bio-based excipients is increasingly encouraged and highly preferred especially in biopolymer composites [14,15]. The substitution of PER with renewable char forming materials (mainly polysaccharides) was found to be an obvious and viable solution to provide greener flame retardant formulations, among others, for PLA [16–21].

Cyclodextrins are cyclic oligosaccharides formed by the enzymatic treatment of starch [22]. Cyclodextrins and their derivatives are widely used in many industrial and scientific fields [23] and gain popularity in the plastic industry as well. Their inclusion complexes of fragrances, antimicrobial and antioxidant agents, dyes, insecticides, UV-filters can be incorporated into polymers either to ensure slow-release or homogeneous distribution of the complexed substances [24] utilised in the packaging industry [25,26] and pharmaceuticals [27,28]. Cyclodextrins have also

* Corresponding author.
E-mail address: kbocz@mail.bme.hu (K. Bocz).

https://doi.org/10.1016/j.polymdegradstab.2021.109655

shown a lot of potential as FR components in multiple polymer systems like epoxies [29,30], elastomers [31–33], polyesters [34,35] polypropylenes [36–40], and other polymeric systems [41–43]. Also, in PLA, β-cyclodextrin (β-CD) has been found to be an effective carbonization agent due to its charring ability and thermal stability. Feng et al. [44] gained a high amount of charred residue in PLA with a 20 wt% β-CD/APP/MA (ratios: 1/2/1) additive system. Teoh et al. [45] showed that in PLA/PMMA system β-CD additive improves the char formation efficiency, as in PLA/PMMA20/FR/β-CD system at 20 wt% additive content with 1:1 FR/β-CD ratio the cyclodextrin suppressed the melt-dripping behaviour and also retained and resisted the loss of phosphorus FR during the polymer combustion. Vahabi et al. [46] synthesised an organic-inorganic hybrid with β-CD (BSDH); and this novel additive has shown to have an excellent synergistic effect in improving the flame retardancy of PLA/APP/BSDH composite, as demonstrated by the significant reduction of peak heat release rate (pHRR) and total heat release (THR) values. Zhang et al. [47] created phospholipidated β-cyclodextrin (PCD) through interfacial polycondensation and found the optimum mass ratio of APP to PCD to be 5 to 1. At this ratio, with 30 wt% loading, the LOI reached 42.6% accompanied with UL-94 V-0 rating, and in mass loss cone calorimetry (MLC) test the highest amount of char residue (71.5 wt%) was obtained besides significant reduction of pHRR and THR values compared to the neat polymer. Even when the total loading of APP and PCD was decreased to 20 wt%, still V-0 rating according to the UL-94 standard was reached.

It has been shown recently that the particle size of the flame-retardant additives has a significant impact on both the flammability and mechanical performance of intumescent flame-retarded compounds. Depending on the (relative) particle size and the dispersion of the components of an IFR system in the polymer matrix, their interaction and reaction pathway can change, and thus carbonaceous chars of different composition and structure can be obtained, significantly differing in flame-retarding performance [48]. Electrospinning (ES) technology has been receiving increasing attention due to its capability to produce ultrafine micro- or nanofibres, or fibrous structures proven to be practical in many fields, even in flame retardancy of materials. Vahabi et al. have recently reviewed the state-of-the-art features of flame-retardant polymer materials developed by using electrospinning [49]. Among others, electrospun nanofiber mats were successfully used as fire protecting coatings [50] or as submicronic additives with simultaneous reinforcing and flame retarding capability [51].

Recently, cyclodextrins (CDs) have been successfully electrospun as CDs are capable of forming polymer-like supramolecular structures via intermolecular interactions [52]. Vass et al. [53,54] manufactured grindable HP-β-CD microfibres with diameters in the range of 2–10 μm with a uniquely high production rate of 270 g/h using aqueous high-speed electrospinning technique. The thus obtainable enhanced specific surface area of the fibrous material provides further benefits and widens the perspectives of cyclodextrin-based formulations.

In this work, microfibrous structures were manufactured from the aqueous solution of 2-hydroxypropyl-beta-cyclodextrin (HP-β-CD) by high-speed electrospinning method and then used as a bio-based charring agent in intumescent flame-retarded PLA. Our hypothesis was that the specific surface area of HP-β-CD plays a role in its flame-retardant efficiency. Therefore, the flame-retardant performance of microfibrous HP-β-CD was compared to that of commercially available powder form in PLA/APP/HP-β-CD systems. Also, the morphological, thermal, and mechanical properties of the flame-retarded biopolymer composites were comprehensively studied.

2. Material and methods

2.1. Materials

Ingeo™ Biopolymer 4032D type extrusion grade poly(lactic acid) (PLA), supplied by NatureWorks LLC (Minnetonka, MN, USA), was used as polymer matrix material. Exolit® AP 422 type ammonium-polyphosphate (APP), received from Clariant AG (Muttenz, Switzerland), was applied as a flame-retardant additive. 2-hydroxypropyl-beta-cyclodextrin (HP-β-CD) (Kleptose® HPB, MS nominal value: 0.62) was obtained from Roquette Pharma (Lestrem, France).

2.1.1. Preparation of HP-β-CD microfibres

The microfibrous HP-β-CD type additive was prepared by high-speed electrospinning (HSES) and subsequent milling. Fig. 1 shows the schematic representation of the preparation steps.

The HSES setup used for fibre formation consists of a stainless steel spinneret (d = 34 mm) connected to a high-speed motor [53]. The disk-shaped spinneret is equipped with 36 equidistantly distributed orifices (d = 330 μm) located in the sidewall of the wheel. For the solution, 68 wt% HP-β-CD was added to purified water and the mixture was stirred with a magnetic stirrer (100 rpm) at room temperature until complete dissolution (24 h). The solutions were fed with a SEP-10 S Plus syringe pump with a flow rate of 350 mL/h. The rotational speed of the spinneret was fixed at 40,000 rpm. The applied voltage was 40 kV during the experiments (Unitronik Ltd., Nagykanizsa, Hungary). The conical bottom of the drying chamber was grounded, and it acted as the counter electrode. Air knives were used to remove the dried material from the surface of the chamber and a constant airflow (120 m^3/h, room temperature) was applied to help the dried fibres to reach the cyclone. The experiments were performed at ambient temperature (25 °C). The produced fibrous material was collected by a cyclone. The high throughput fibre forming technology enabled the production of HP-β-CD microfibres with uniquely high productivity of 270 g/h. The obtained electrospun material was then ground to make it suitable for blending with excipients. For this purpose, a hammer mill (IKA MF10, IKA-WERKE GmbH & Co. KG, Staufen, Germany) was used with a 1.0 mm sieve at 3000 rpm. Including the dissolution, spinning, collecting, and grinding losses, a 76% yield was obtained.

Based on the SEM images presented in Fig.1 with identical magnifications of 100×, the morphology of the inherent powder form of HP-β-CD can be compared with that of the obtained fibrous form. The obvious reduction in particle size is accompanied by an approximately 9-fold increase in the surface area to volume ratio, as estimated by image processing of SEM micrographs (see in 2.3.1.1 paragraph), which was expected to be relevant regarding the performance in the IFR system.

2.2. Preparation of flame-retarded PLA composites

2.2.1. Mixing

The flame-retarded PLA composites were prepared using a Brabender Plasti-Corder Lab-Station coupled with W 50 EHT 3Z type internal mixer (Brabender GmbH & Co. KG, Duisburg, Germany) in 50 g batches. Before processing, the raw materials were dried in an oven at 80 °C for 6 h in each case. The internal mixer operated at 180 °C with a continuous rotor speed of 50 rpm. In each case, the polymer mixture was prepared by first adding the pre-measured amount of poly(lactic acid) granules and after adding the additives (15 wt% APP, 3 wt% HP-β-CD) and then mixed for 10 min. In Table 1 the compositions of the prepared flame-retarded PLA composites are shown.

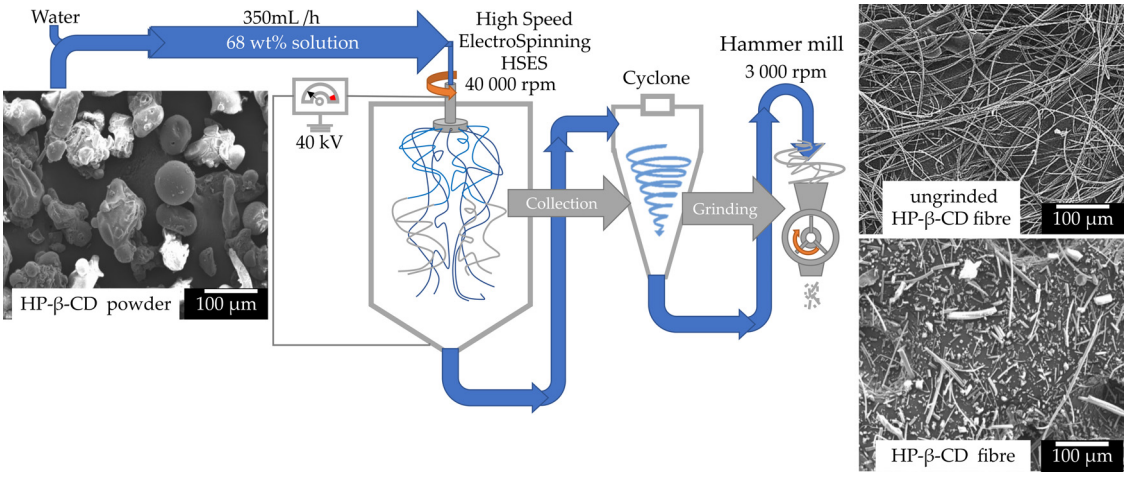

Fig. 1. Preparation of the microfibrous HP-β-CD additive.

Table 1
Formulations of the PLA composites.

Sample name	PLA [wt%]	APP [wt%]	HP-β-CD powder [wt%]	HP-β-CD fibre [wt%]
PLA	100%	–	–	–
PLA/APP	85%	15%	–	–
PLA/APP/HP-β-CD powder	82%	15%	3%	–
PLA/APP/HP-β-CD fibre	82%	15%	–	3%

The ratio of APP to HP-β-CD was chosen based on the results of Zhang et al. [47], who found the APP to PCD mass ratio of 5 to 1 to be optimal regarding the flame retardant efficiency of the system. For comparison, also test specimens from neat PLA and PLA containing only APP were also manufactured and examined.

2.2.2. Moulding

The mixed materials were dried overnight at 70 °C and then hot-pressed using a Teach-Line Platen Press 200E heated platen press (Dr. Collin GmbH, Munich, Germany). About 30 g of each mixed sample was heated to 180 °C in a mould of 100 × 100 × 2 mm^3 size, then the plates were compressed for 4 min with the gradual addition of pressure up to 100 bars and finally cooled to 50 °C under pressure. The specimens for flammability and mechanical testing were obtained by cutting the plates with a disk saw. Prior to performing the experiments, the test specimens were stored in sealed bags at room temperature.

2.3. Characterisation methods

2.3.1. Scanning electron microscopy

Scanning electron microscopic (SEM) micrographs of the powder and electrospun HP-β-CD and the cryogenic fracture surface of the flame-retarded PLA samples were taken using a 6380LVa (JEOL, Tokyo, Japan) type apparatus in high vacuum at an accelerating voltage of 10 keV. Before the examination, all the samples were fixed by conductive double-sided carbon adhesive tape and sputtered by gold using ion sputter (JEOL 1200, JEOL, Tokyo, Japan) to prevent charge build-up on the surface.

2.3.1.1. Determination of specific surface area of the HP-β-CD additives. Particle sizes and the specific surface area of the HP-β-CD additives were determined by image processing of SEM micrographs with 100× magnification using MATLAB's (The MathWorks, Inc., Natick, MA, USA) Image Processing Toolbox. In the SEM images (Fig. 2), the outline of the identified particles was selected (at least 100 for each type of particle), from which the size values were calculated.

The program calculated the area of the particles, from this area the diameter of a circle of equal projection area (d_{EC}, diameter of a circle with an equivalent area of the measured particles) was determined. Then, the maximum diameter (d_M) was measured, that is the longest distance between any two points along the selected boundary. For the calculation of the aspect ratio (A_r), the minimal diameter (d_m) was estimated from a rectangle with the same area as the particle and the length of which is d_M (Fig. 3).

2.3.2. Thermogravimetric analysis

Thermogravimetric analysis (TGA) measurements were carried out using a TA Instruments Q5000 apparatus (TA Instruments LLC, New Castle, NH, USA) under 25 mL/min nitrogen gas flow. Samples of about 10 mg were positioned in open platinum pans. The polymer samples were heated from 25 °C to 800 °C with a 10 °C/min rate (The precision on the temperature measurements is ±1.5 °C in the temperature range of 25–800 °C.)

2.3.2.1. Determination of residual water content. To determine the residual water content of the HP-β-CD samples, thermogravimetric analyses were carried out with the same Q5000 type TGA instrument (TA Instruments, New Castle, DE, USA) under nitrogen atmosphere. The samples were heated up from 25 to 105 °C with a 2 °C/min ramp and then kept at 105 °C for 20 min to reach mass constancy. Then the heating cycles were continued up to 800 °C with a heating speed of 10 °C/min to examine the degradation processes. During the measurements, the applied nitrogen flush was 25 mL/min.

2.3.3. Tensile tests

Comparative tensile tests were performed on rectangular specimens of 100 × 10 × 2 mm^3 (width × length × depth) (the gauge length was 60 mm) using a Zwick Z020 universal tester (Zwick GmbH & Co. KG, Ulm, Germany) with a crosshead speed

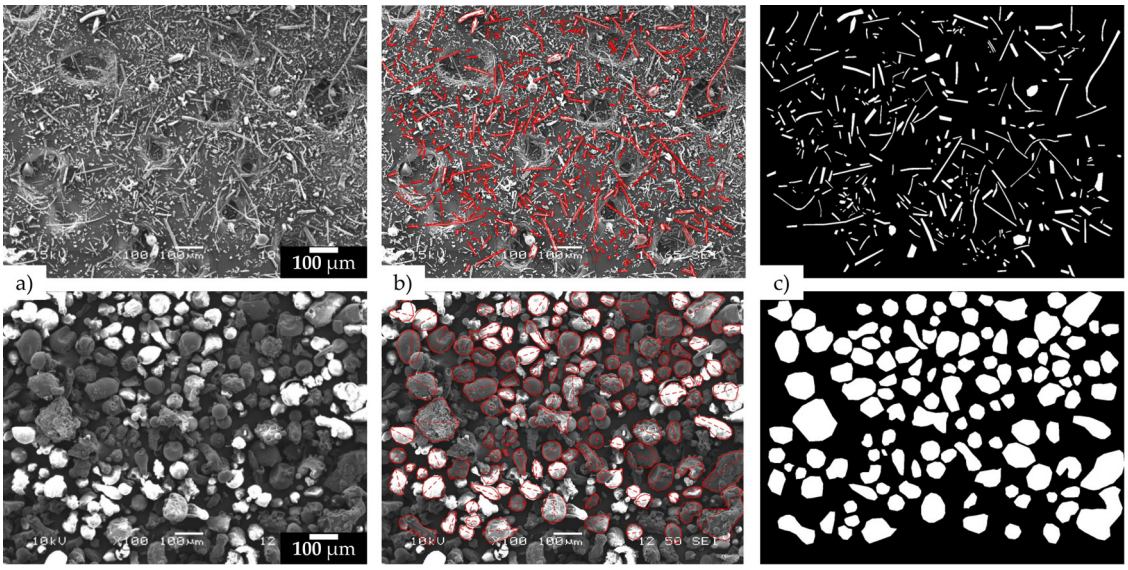

Fig. 2. The steps of the particle size distribution measurement: (a) The SEM image, (b) the selected circumference of the particles and their maximum diameter (c) area of selected particles in the binary image.

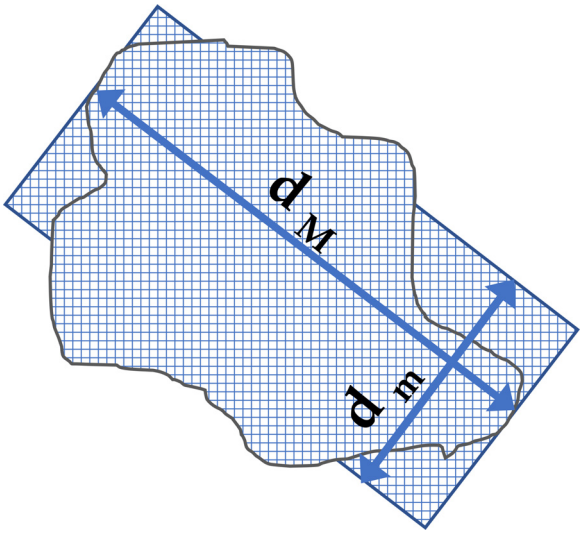

Fig. 3. The estimation of the minimal diameter (d_m), the width of a rectangle with maximum diameter (d_M) length and the same area as the particle.

of 5 mm/min. 5 specimens were tested from each composite sample. Before the measurements, the exact thickness and width of each specimen were measured with a calliper. Based on the measured geometric data and the resulting stress-strain curves, tensile strength (σ_M), Young's modulus (E), and the relative elongation at maximum force (ε_M) were calculated for each specimen using the ISO 527-1:2012 standard.

2.3.4. Differential scanning calorimetry

For the differential scanning calorimetry (DSC) measurements, a DSC 3+ type device (Mettler Toledo, Greifensee, Switzerland) was used. Approximately 10 mg of the samples were weighed into aluminium crucibles with pre-punched tops. The encapsulated samples were then placed on the measuring cell by the automatic sample dispenser of the instrument. During the analysis, the samples were first heated from 25 °C to 200 °C at 10 °C/min, then cooled from 200 °C to 25 °C at 2 °C/min, and then again heated at 10 °C/min rate from 25 °C to 200 °C. The thermal data was analysed with STAR^e Evaluation Software (Mettler Toledo, Greifensee, Switzerland). The degree of crystallinity (χ_c) of the samples was calculated according to Eq. (1), where ΔH_m indicates the melting enthalpy, ΔH_c is the cold crystallization enthalpy, ΔH_m^0 is the melting enthalpy of the 100% crystalline PLA equal to 93.0 J/g, and ϕ is the weight fraction of the additives.

$$\chi_c(\%) = \frac{\Delta H_m - \Delta H_c}{(1-\phi)\Delta H_m^0} \times 100\% \quad (1)$$

2.3.5. Limiting oxygen index

Limiting oxygen index (LOI) was determined on specimens with 100 × 10 × 2 mm^3 dimensions according to ISO 4589 standard using an apparatus made by Fire Testing Technology Ltd. (East Grinstead, West Sussex, UK).

2.3.6. UL-94

Standard UL-94 flammability tests were performed according to ISO 9772 and ISO 9773, the specimen dimensions for the test were 100 × 10 × 2 mm^3.

2.3.7. Mass loss calorimetry

Mass loss type cone calorimeter (MLC) tests were carried out by an instrument delivered by Fire Testing Technology Ltd. (East Grinstead, West Sussex, UK) using the ISO 13927 standard method. Specimens (100 × 100 × 2 mm^3) were exposed to a constant heat flux of 35 kW/m^2, simulating a mild fire scenario. The ignition was provided by a spark plug located 13 mm above the sample. The main characteristic of fire properties, including heat release rate (HRR) as a function of time, time to ignition (TTI), and total heat release (THR), were determined. When measured at 35 kW/m^2, HRR and THR values were reproducible to within ±10%.

From the collected data Flame Retardancy Index (FRI) was calculated according to the following formula [55]:

$$FRI = \frac{\left[THR*\left(\frac{pHRR}{TTI}\right)\right]_{Neat\ Polymer}}{\left[THR*\left(\frac{pHRR}{TTI}\right)\right]_{Composite}} \quad (2)$$

2.3.8. Mechanical characterisation of chars

To determine the structural and mechanical properties of the carbonaceous residue remaining after combustion of the polymer samples, Advanced Rheometer AR 2000 (TA Instruments, New

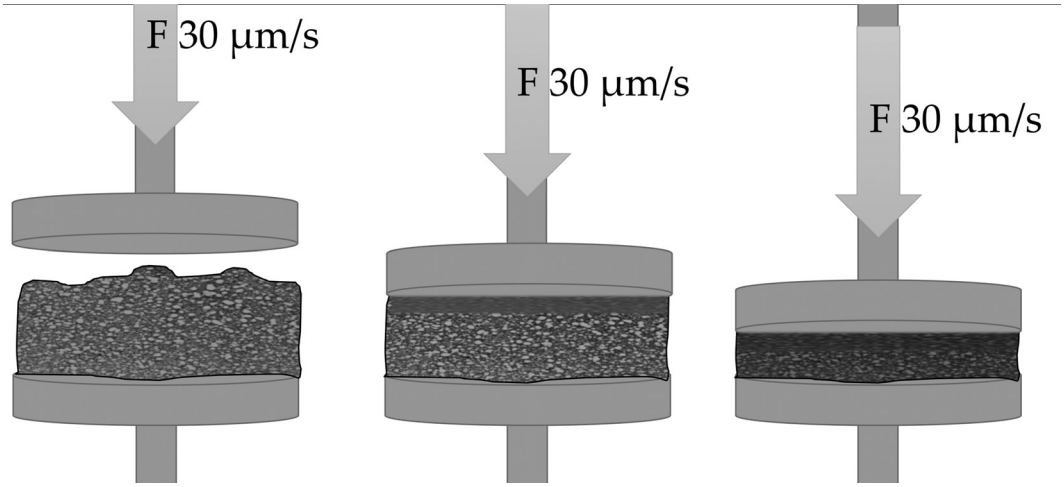

Fig. 4. Schematic representation of the char compression test.

Table 2
Measured and calculated size parameters of the HP-β-CD particles.

Property	Unit	HP-β-CD powder	HP-β-CD fibre
Average d_{EC}	[µm]	64 ± 22	15 ± 8
Average d_M	[µm]	80 ± 31	38 ± 35
Average area	[µm^2]	3580 ± 2678	232 ± 261
Aspect ratio	[-]	0.54 ± 0.11	0.25 ± 0.18
Surface to volume ratio	[1/µm]	0.09	0.84

Castle, DE, USA) equipment was used. For the measurements, 40 × 40 × 3 mm^3 polymer samples were burnt under the cone heater of the MLC at a heat flux of 35 kW/m^2 until the carbonaceous layer formed and smoke formation stopped. The mechanical resistance of the charred residues was evaluated according to the method used in previous studies [56]. The charred samples were then placed between two 25 mm diameter metal plates, the lower was fixed while the upper plate compressed the samples with a constant speed of 30 µm/s (Fig. 4).

Upon compression, the normal force required to exert continuous movement transduced by the charred layer was constantly detected and registered.

3. Results and discussion

Two types of HP-β-CD additive, differing in particle size and aspect ratio, i.e. commercially available powder and electrospun microfibres, were used as biobased charring agents at 3 wt% loadings besides 15 wt% APP in PLA matrix thus setting the 5:1 mass ratio of APP to CD also found to be optimal by Zhang et al. [47]. The potential role of the morphology of the used HP-β-CD was comprehensively investigated on the thermal, flammability, and mechanical properties of the flame-retarded PLA composites, as well as on the evolution of the intumescent flame-retardant system.

3.1. Determination of specific surface area of the HP-β-CD additives

From the data acquired from the analysis of the SEM images taken of the two types of HP-β-CD particles, the average surface to volume area was estimated for both additives. The average values of d_{EC} and d_M, the average size of the marked areas, as well as the calculated surface to volume ratios are reported in Table 2. The specific surface area of the powder particles was estimated using the d_{EC}. In the case of the fibrous material the d_M value, the average length and diameter were considered to calculate an average specific surface area. Accordingly, a 9-fold increase in the surface area to volume ratio of the HP-β-CD particles was achieved by fibre formation using the aqueous HSES method.

3.2. Thermogravimetric analysis of the additives

The thermal behaviour of the used flame-retardant additives was investigated by thermogravimetric analyses performed in N_2 atmosphere. The resulting thermograms are shown in Fig. 5, while the main thermal characteristics are summarised in Table 3. For comparison, the TGA thermogram and relevant data corresponding to neat PLA are also presented. It can be observed that the decomposition of PLA occurs nearly in the same temperature range (290 to 310 °C) as the first decomposition step of APP. For HP-β-CD samples, the initial weight loss up to 100 °C is due to the loss of absorbed water and water of crystallisation [57] which was measured to be 4.5 wt% for the powder and 7.9 wt% for the fibrous material. The significantly increased amount of absorbed water detected in the case of the microfibrous HP-β-CD is associated with its noticeably increased surface area, obtained as a result of fibre formation.

The second weight-loss step of the β-cyclodextrins, occurring at around 335 °C is related to their single step decomposition, resulting in a carbonaceous residue (char). The decomposition of the fibrous HP-β-CD begins at a slightly higher temperature and occurs at a lower rate compared to the powdered form. The last degradation stage (T > 400 °C) corresponds to the slow rate degradation of the char. It can be observed, however, that a noticeably higher amount of residue remains at 800 °C from the fibrous HP-β-CD (5.9 wt%) than that from the powder HP-β-CD (1.2 wt%) indicating increased thermal stability of the charred residue that forms from the cyclodextrin with a fibrous supramolecular structure.

3.3. Scanning electron microscopy of the composites

SEM micrographs, taken from the cryogenic fracture surfaces of the flame-retarded PLA composites, are presented in Fig. 6. In the image of PLA/APP composite, particles stuck together, and detached boundaries of APP particles between APP and PLA (Fig. 6a). Similarly, due to the strong polarity of HP-β-CD, poor interfacial interaction is expected in the HP-β-CD containing PLA composites as well. On the contrary, in Fig. 6b and c, the better dispersion and less sharp phase boundaries of APP particles can be recognised suggesting improved interfacial interaction between APP and the polymer matrix when HP-β-CD is also present in the system. It is proposed that during melt processing the HP-β-CD particles may

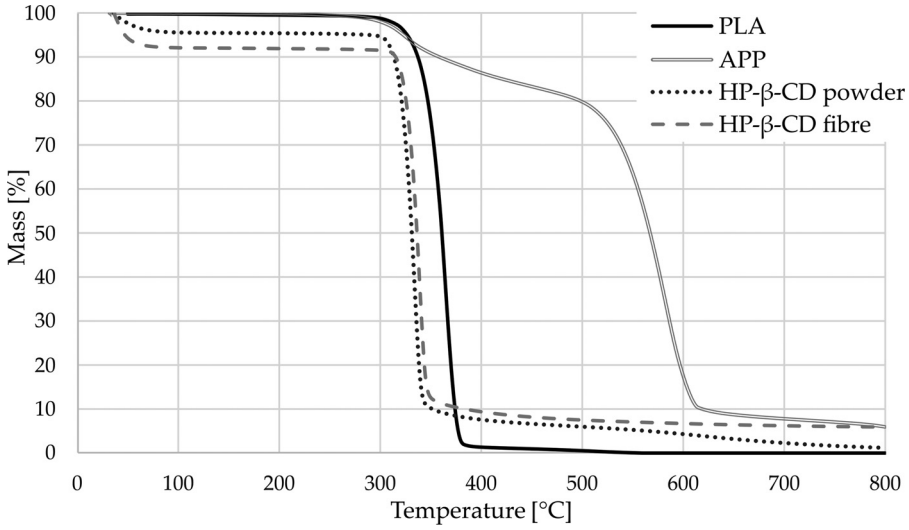

Fig. 5. Thermogravimetric analysis (TGA) curves of poly(lactic acid) (PLA), APP and HP-β-CD powder and fibre additives as measured under N2 atmosphere with the heating ramp of 10 °C/min.

Table 3
Thermogravimetric analysis (TGA) results of the flame-retardant components.

Sample	5% weight loss [°C]	Maximum degradation speed [%/ °C]	Temperature of maximumdegradation speed [°C]	Residue at800 °C [wt%]
PLA	327	3.5	365	0.0
APP	323	0.2/1.1*	325/583*	5.9
HP-β-CD powder	313	4.5	334	1.2
HP-β-CD fibre	320	4.4	339	5.9

***two degradation steps consecutively**.

Table 4
The TGA results of the composites.

Sample	5 wt% loss temperature [°C]	Maximum degradation speed [%/°C]	Temperature of maximum degradation speed [°C]	Residue at 800 °C [wt%]
PLA	327	3.5	365	0.0
PLA/APP	339	2.5	372	5.2
PLA/APP/HP-β-CD powder	329	2.6	368	2.5
PLA/APP/HP-β-CD fibre	327	2.3	371	6.9

allocate around the APP surface and act as a surface modifier. A similar phenomenon was revealed by Yin et al. [58], namely that cellulose nanofibres (CNFs) improve the dispersion of APP within the PLA matrix by acting as interfacial adhesion agent. In this relation, the high-surface-area HP-β-CD microfibres are able to form more physical and also chemical interaction with the APP particles.

3.4. Thermogravimetric analysis of the composites

The thermal characteristics of the PLA composite samples, as measured by TGA in nitrogen atmosphere, are reported in Fig. 7 and Table 4, respectively. It can be seen from the presented results that there is no significant difference between the first decomposition stage of the composites; 5% weight loss can be observed at around 325–340 °C in all cases. The temperature of the maximum decomposition rate does not show a significant difference either. Nevertheless, the lowest maximum degradation rate corresponds to the fibrous HP-β-CD containing sample, while for the sample containing HP-β-CD powder similar value was measured than for the HP-β-CD free PLA/APP sample. Based on this observation, during thermal degradation, a higher degree of interaction is assumed to occur between APP and the microfibrous cyclodextrin. Upon changing the type (i.e. size and structure) of the HP-β-CD used, there is also a difference in the thermal stability and the amount of the residue obtained at 800 °C. In the enlarged part of the figure, it can be seen that above 500 °C, when the second decomposition step of APP occurs, the weight loss is smaller when fibrous HP-β-CD is also present in the system. Above 600 °C, the decomposition of the powder containing sample also accelerates, resulting in less residual mass than remains from the PLA/APP sample. In contrast, the residual weight of the sample containing 3 wt% HP-β-CD in fibrous form remains above the weight of the sample containing only APP even up to 800 °C, thus showing greater thermal stability of the formed char. Based on the TGA analyses performed on the PLA composites it was concluded that the microfibrous structure of the HP-β-CD type bio-based charring agent advantageously influence its interaction with APP and promotes the char formation accompanied with increased thermal resistance that may be crucial regarding the fire protection performance of the intumescent system.

3.5. Differential scanning calorimetry (DSC)

Differential scanning calorimetry (DSC) measurements were used to analyse the polymer phase transitions and calculate the per cent crystallinity of the prepared flame-retarded PLA samples. The main calorimetric data are given in Table 5. Comparing the results of the composites, it can be noticed that during the cooling

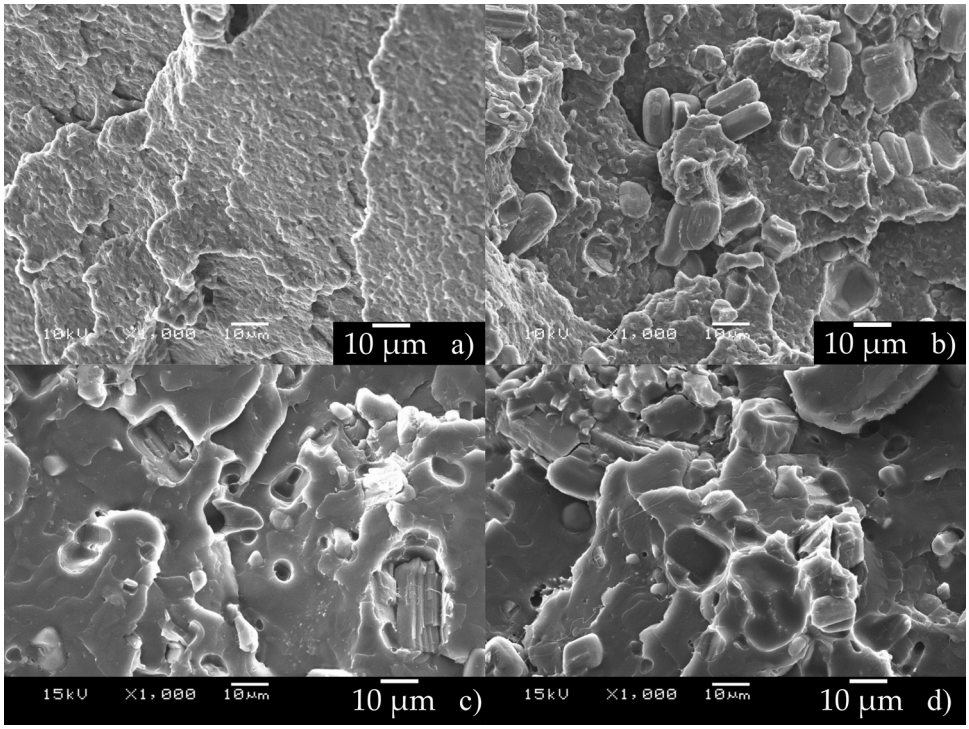

Fig. 6. Scanning electron microscopic images of fracture surfaces with 1000× magnification: a) PLA, b) PLA/APP, c) PLA/APP/HP-β-CD powder and d) PLA/APP/HP-β-CD fibre.

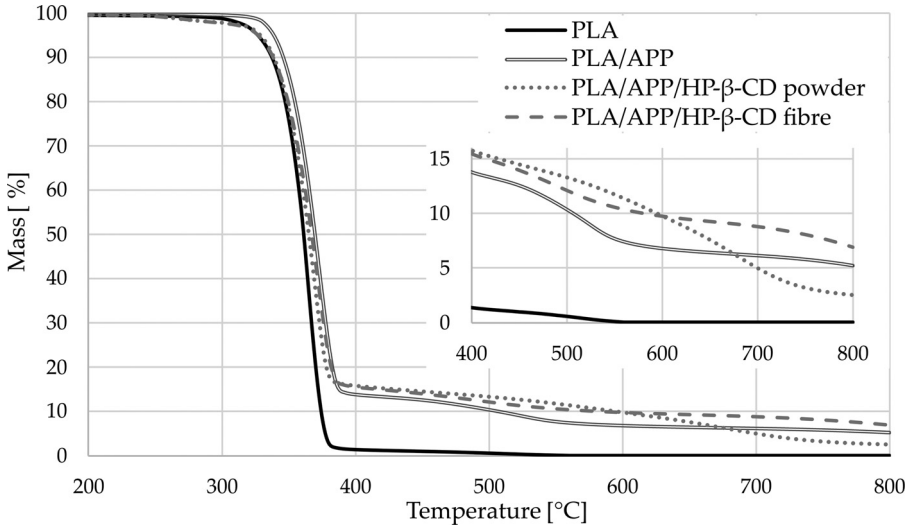

Fig. 7. The thermogravimetric curves of the biopolymer composites (heating rate 10 °C/min, N2 atmosphere).

Table 5
Summary of the DSC thermal data of the PLA composite materials.

Thermal property	Symbol and unit	PLA	PLA/APP	PLA/APP/HP-β-CD powder	PLA/APP/HP-β-CD fibre
Recrystallisation enthalpy [a]	ΔH_c [J/g]	3.7	2.5	3.2	3.2
Melting enthalpy [a]	ΔH_m [J/g]	45.0	32.4	31.3	30.2
Crystallinity [a]	[%]	52.4	44.1	45.2	43.8
Cooling crystallization heat [b]	ΔH_c [J/g]	1.7	19.1	20.2	26.6
Cooling crystallization peak [b]	T_c [°C]	110	101	103	116
Melting temperature [c]	T_m [°C]	168	169	169	168
Glass transition temperature [c]	T_g [°C]	62	63	64	64
Melting enthalpy [c]	ΔH_m [J/g]	13.5	28.7	28.0	29.3
Crystallinity [c]	[%]	14.5	36.3	36.7	38.4

[a] denotes the first DSC run (heating).
[b] denotes the second DSC run (cooling).
[c] denotes the third DSC run (heating) in heat/cool/heat DSC procedure.

Table 6
Tensile test results of the composite samples.

Sample name	Tensile strength E [MPa]	Young's modulus σ_M [MPa]	Elongation at yield ε_M [%]
PLA	61.0 ± 2.5	3125 ± 106	2.7 ± 0.3
PLA/APP	42.9 ± 2.4	3123 ± 125	2.5 ± 0.5
PLA/APP/HP-β-CD powder	34.5 ± 2.4	2985 ± 127	2.0 ± 0.2
PLA/APP/HP-β-CD fibre	36.8 ± 2.2	3171 ± 147	2.2 ± 0.2

Table 7
The results of LOI and UL-94 tests on the control and composite samples.

Sample	LOI [%]	t_1/t_2 [s]*	UL-94 Cotton ignition	Rating
PLA	20.5	-/ -	–	H.B. 34 mm/min
PLA/APP	26.0	3/1	yes	V-2
PLA/APP/HP-β-CD powder	29.0	2/1	yes	V-2
PLA/APP/HP-β-CD fibre	32.5	4/1	yes	V-2

*represent the after-flame time after the flame application of first and second 10 s, and "-" means complete combustion for samples.

of the fibrous HP-β-CD containing sample, crystallization of PLA started at a noticeable higher temperature (T_c = 116 °C), which indicates increased nucleating effect of the high-surface-area cyclodextrin. It can also be seen that for all the three flame-retarded composites, the crystallinity determined from the second heating cycle increased compared to the additive-free PLA, which can be connected to the decrease in molecular weight due to high temperature and shear forces occurring during the production of the composites [59].

3.6. Tensile tests

Tensile tests were performed to study the effect of the used FR components on the mechanical performance of the PLA composites. In Table 6, the tensile strength, Young's modulus and elongation at yield values measured for the flame-retarded PLA composites are presented. As expected, both neat APP and HP-β-CD act as a non-reinforcing filler in the PLA matrix and result in decreased tensile strength and elongation. Comparing the effects of powder and fibrous HP-β-CD, it can be concluded that using fibrous HP-β-CD slightly better results can be obtained with respect to all the studied mechanical properties (higher modulus, strength and elongation) than with the conventional powder additive. Based on this result it is presumed that the microfibrous HP-β-CD, due to its small particle size and high aspect ratio, can have a reinforcing effect in the system. Also, the surface modifying the efficacy of the microfibrous HP-β-CD is believed to be higher than that of the conventional powder form that results in increased interfacial compatibility between APP and PLA enabling more efficient transfer of external loads from the polymer matrix to the fillers.

Analysis of variance (ANOVA) was performed to evaluate the effect of the used FR additives on Young's modulus. Results indicated that the type of the additive has no significant influence on this mechanical characteristic (p-value = 0.114, significance level: 5%). However, by performing planned comparisons with contrast coefficients it was confirmed that there is a significant difference between the modulus values of PLA/APP/HP-β-CD powder and PLA/APP/HP-β-CD fibre samples (p-value = 0.0233, significance level: 5%). Accordingly, it can be concluded that the particle size and structure of the HP-β-CD used at 3 wt% has an effect on the modulus of the flame-retarded composite.

3.7. Limiting oxygen index and UL-94

The results of the LOI and UL-94 measurements performed on the flame-retarded PLA composites are summarized in Table 7. In the case of PLA without flame retardants, during performing the horizontal test the flame spread throughout the test specimen, the average flame spreading rate was calculated to be 34 mm/min.

In the case of the sample with APP alone, a minimal level of charring was observed, while in the case of the specimens combined with HP-β-CD, the phenomenon of charring was more visible. Comparing the powder and fibrous HP-β-CD containing samples, it was observed that on the surface of the out flamed specimens with fibrous HP-β-CD somewhat more carbonaceous char formed. However, apart from this, for each sample, the falling polymer droplets ignited the piece of cotton wool placed underneath, thus achieving a V-2 rating according to the UL-94 standard.

The measured LOI values show that both types of HP-β-CD, when applied at 3% besides 15% APP, effectively increase the LOI of the PLA composites. Nevertheless, it was found, that the LOI of the flame-retarded PLA composite containing fibrous HP-β-CD is significantly higher than that of the sample containing the same amount of HP-β-CD powder. Consequently, the smaller particle size and increased surface area to volume ratio of the fibrous cyclodextrin is believed to be of key importance regarding its flame retardant efficiency.

3.8. Mass loss calorimetry

The heat emission curves gained from the Mass Loss calorimeter measurements of the PLA composites are shown in Fig. 8 while the recorded mass loss during the combustion is presented in Fig. 9. Main flammability characteristics are summarised in Table 8. Based on the heat emission curves it can be seen that the HP-β-CD type charring agents greatly reduced the amount of heat emitted during the combustion of the PLA composites. Compared to the PLA/APP sample, the heat release rate curves are flatter and more elongated in time when HP-β-CD is also present in the system. This slower decomposition phenomenon can also be read when comparing the slope of the weight loss curves in Fig. 9.

The samples containing FR additives show a 20–25% lower total heat release (THR) compared to neat PLA. The peak heat release rate (pHRR) values show a similar decrease. For both measured quantities, the sample containing fibrous HP-β-CD showed the best results with a 25% reduction in total heat emission and a 40% reduction in the peak heat release rate compared to those of neat PLA. The maximum rate of heat emission (pHRR) corresponding to the sample containing fibrous HP-β-CD was also significantly (by 33%) lower compared to the PLA/APP system, and also the highest amount of carbonaceous residue ($m_{residue}$) was formed from

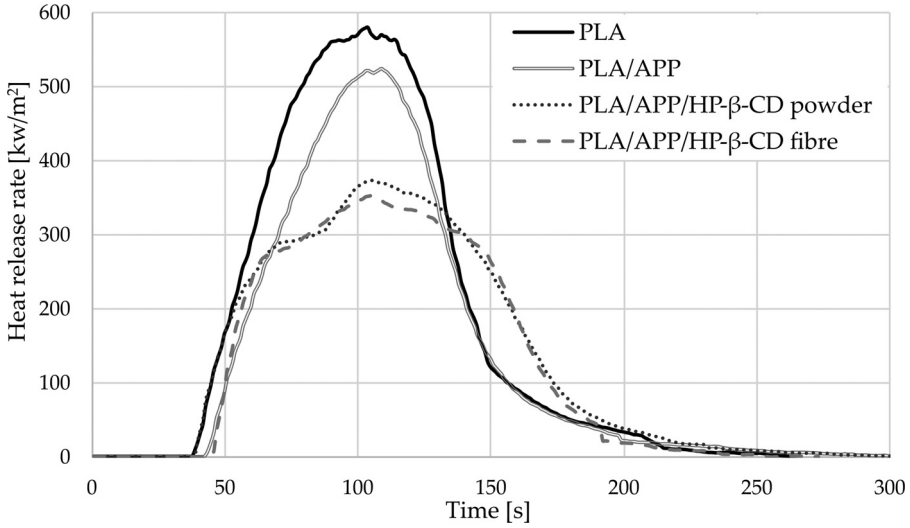

Fig. 8. Heat release curves of polymer samples over time.

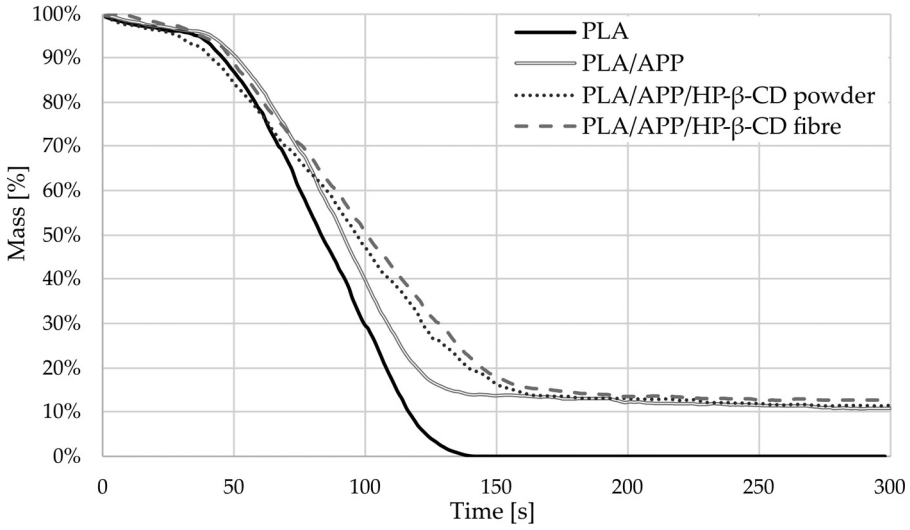

Fig. 9. Mass loss of polymer samples over time.

Table 8
Combustion characteristics obtained from MLC tests and the calculated Flame Retardancy Index (FRI).

Sample name	t_{ign} [s]	pHRR [kW/m²]	t_{pHRR} [s]	THR [MJ/m²]	$m_{residue}$ [%]	FRI [-]
PLA	38 ± 4	581 ± 7	104 ± 2	47.2 ± 0.3	0.0 ± 0.0	1.00
PLA/APP	43 ± 4	525 ± 3	109 ± 1	39.7 ± 0.8	10.6 ± 0.2	1.49
PLA/APP/HP-β-CD powder	39 ± 1	374 ± 9	105 ± 1	38.8 ± 0.5	10.6 ± 0.4	1.94
PLA/APP/HP-β-CD fibre	45 ± 4	353 ± 19	105 ± 1	35.8 ± 0.9	11.9 ± 0.4	2.57

this sample. Based on the Flame Retardancy Indices (FRIs) of the composites, both HP-β-CD containing IFR systems provide "good" flame retardant performance ($1 < FRI < 10$) [55]. Nevertheless, FRI increased from 1.94 (with powder HP-β-CD) to 2.57 (with microfibrous HP-β-CD) only by changing the physical form i.e. the specific surface area of the used HP-β-CD. It was concluded that the microfibrous structure of the charring agent is beneficial regarding the flame retardancy performance of the IFR system. The charred residues obtained after cone calorimeter tests show slightly differing morphology, as can be seen in Fig. 10. It is proposed that the well-dispersed microfibrous HP-β-CD improves the integrity of the intumescent char layer, thereby improving its thermal and mechanical stability and thus contributes to better flame retardation. To further investigate this phenomenon, the mechanical resistance of the carbonaceous residues was analysed with compression tests.

3.9. Mechanical characterisation of chars

The thickness, structure and mechanical stability of the intumescent chars are crucial regarding their fire protecting performance. The mechanical resistance of the chars formed from the flame-retarded PLA composites containing HP-β-CD as charring agents were compared by performing compression tests. As the heights of the examined chars were different, in Fig. 11 the registered normal force values obtained from three parallel measurements were plotted against the percentage of deformation of the corresponding chars. To characterize the mechanical resistance of

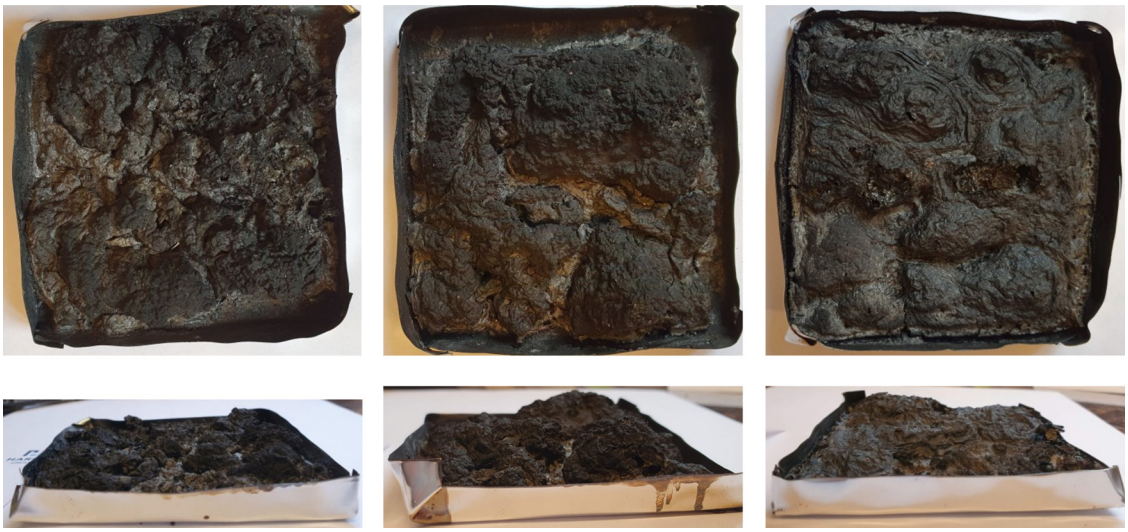

Fig. 10. The charred residues obtained after cone calorimeter tests from left to right: PLA/APP; PLA/APP/HP-β-CD powder; PLA/APP/HP-β-CD fibre.

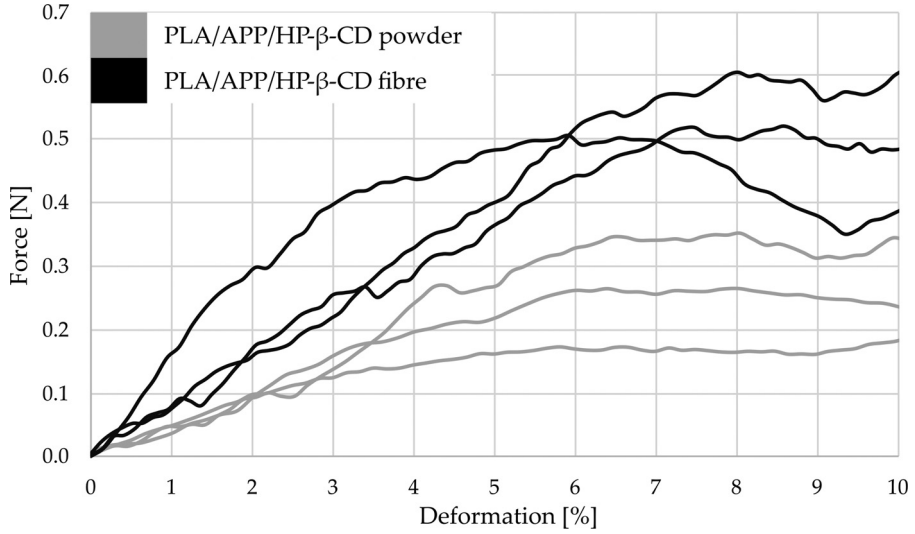

Fig. 11. Normal force vs. deformation curves measured for the chars formed from the two types of HP-β-CD containing intumescent flame-retarded systems.

Table 9
Initial height, maximum strength (on 0–10% deformation interval), modulus and strength of the charred residues.

Sample	Initial height [mm]	Strength [Pa]	Modulus [kPa]	Char strength [Pa/def%]
PLA/APP/HP-β-CD powder	17 ± 2	542 ± 142	9.6 ± 2.5	4.7 ± 1.1
PLA/APP/HP-β-CD fibre	22 ± 2	1107 ± 88	18.8 ± 2.6	8.2 ± 1.0

the foam structures, the char strength and modulus values were calculated for each tests sample, which can be seen in Table 9 together with the determined initial heights of the examined intumescent char layers. The presented mechanical characteristics can be interpreted as the resistance of the formed carbonaceous residue to deformation. The combustion residues corresponding to the fibrous HP-β-CD containing sample showed improved resistance to deformation even though these char layers had a larger extent (thickness reached nearly 2 cm). The compression strength of the carbonaceous residue corresponding to the PLA/APP/HP-β-CD fibre sample (1107 ± 88 Pa) was measured to be more than two-fold greater than that of the sample containing identical amount of conventional powdered HP-β-CD (542 ± 142 Pa). The fibrous HP-β-CD was found to similarly increase the stiffness (modulus) of the charred layers. The thermal and mechanical resistance of an intumescent char fundamentally determines the flame retardant effectiveness of the protective layer. Our results show that the microfibre-structured HP-β-CD effectively strengthens the carbonaceous layer, thereby improving its heat and material transport inhibitory effect. The key importance of compact char formation is more obvious when the ignition source comes from the edges of samples (e.g. LOI test), where the efficient barrier against heat, oxygen and fuel transport can result in immediate fire extinction.

The microstructure of the charred residues was also examined by SEM. In Fig. 12, micrographs with a magnification of 100× are presented, showing the characteristic pore structure of a relatively large area. Accordingly, the multicellular honeycomb structure is characteristic for both chars, however, they differ in pore size; the

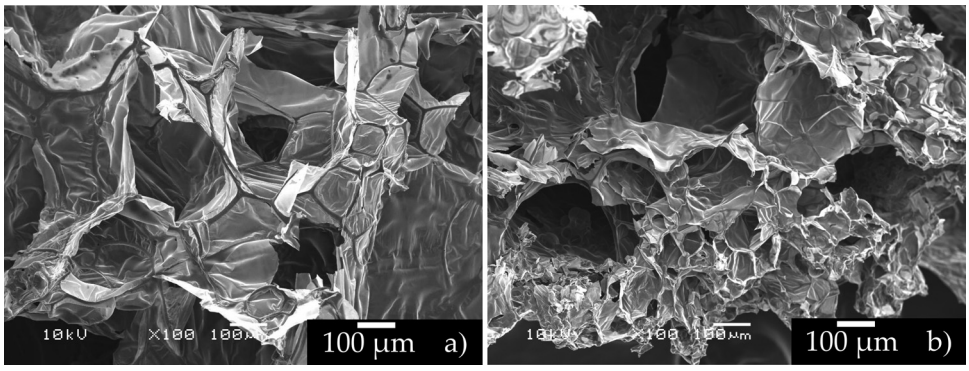

Fig. 12. SEM images of the char residues; a) PLA/APP/HP-β-CD powder, b) PLA/APP/HP-β-CD fibre.

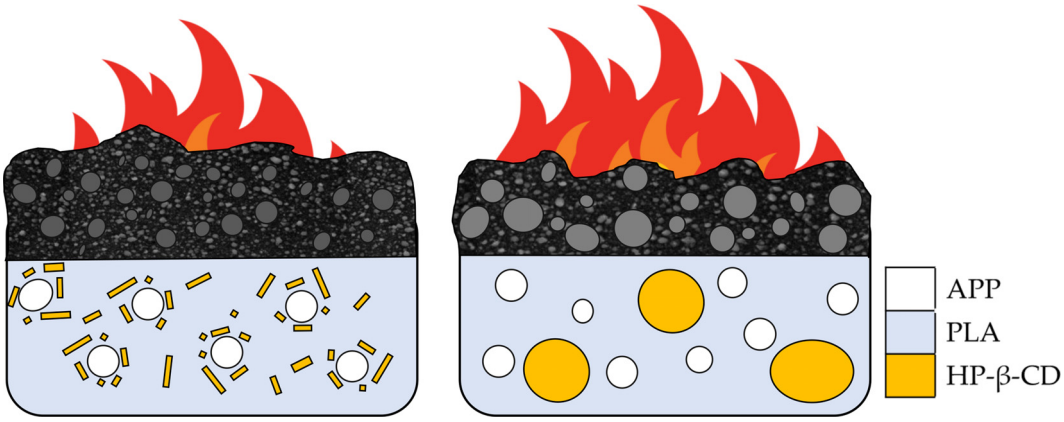

Fig. 13. Schematic representation of the flame retardancy mechanism.

charred residue corresponding to the fibrous HP-β-CD containing composite is composed of noticeably smaller cells. It is proposed that the high-surface-area HP-β-CD microfibres may initiate cell nucleation during the simultaneous charring and expansion process, resulting in higher cell density. The increased APP/HP-β-CD interaction proposed based on Figs. 6 and 7, may have a similar effect during intumescent char forming. At a comparable expansion ratio, with a smaller cell diameter and a greater number of cells the amount of heat absorbed and scattered by the walls during the heat transfer process increases, which results in smaller heat conductivity. The greater initial heights of the carbonaceous layers of the PLA/APP/HP-β-CD fibre samples are also associated with lower heat conductivity. As both parameters, i.e. smaller cell size and increased thickness, are positively correlated with thermal insulation, they are important factors in providing improved flame retardancy as well.

4. Conclusion

It is demonstrated that the efficiency of an intumescent flame-retardant system can be noticeably improved just by reducing the particle size and aspect ratio of the used charring agent. In this study, the specific surface area of HP-β-CD was increased ninefold by the high throughput aqueous HSES fibre forming technology. The thus obtained high-surface-area HP-β-CD microfibres were found to have better char promoting performance in intumescent flame-retarded PLA system than the conventional HP-β-CD powder. By increasing the specific surface area of the used charring agent, a remarkable increment of the LOI value (from 29.0% to 32.5%) and a noticeable improvement in all the combustion characteristics, measured by cone calorimeter tests, were achieved. Furthermore, the investigated mechanical characteristics of the flame-retarded PLA composites also improved when the HP-β-CD additive was used in a microfibrous form.

The improved flame retardant performance of the microfibrous charring agent is proposed to rely on multiple effects. On one hand, it was evinced by TGA analyses that the associated supramolecular structure of the electrospun HP-β-CD fibres is thermally more stable than the powdered form, so is the char that remains after decomposition of the fibrous material. On other hand, based on SEM imaging and mechanical characterisation of the composites, HP-β-CD particles tend to allocate around the APP particles during melt processing when the high-surface-area microfibres are able to form more interactions with the acid source. As a result, the char formation will be more effective, as indicated by the increased amount of residue obtained both after TGA analysis and cone calorimeter test. Besides these effects, the microfibres are believed to have an increased cell nucleating effect during the swelling process, resulting in a honeycomb structured char that is composed of smaller cells accompanied by lower thermal conductivity. Also relating to this effect, the char layer formed from the fibrous HP-β-CD containing PLA composite was found to have about two times higher compression strength and modulus than those of the powdered HP-β-CD containing composite. By this means, an advantage of various microfibrous fillers, namely that they can reinforce the intumescent char layer without compromising its expandability, has been successfully utilised with the cyclodextrin type charring agent. As a consequence of all these, by using HP-β-CD with microfibrous structure, an increased amount of intumescent char forms that is thermally and mechanically more resistant and thus provides improved fire protection to the polymer. The proposed flame retardancy mechanism is also presented schematically in Fig. 13.

The new recognition, namely that the particle size reduction of the HP-β-CD type charring agent alone can provide a significant

improvement in the flame retardant efficiency and even in the mechanical properties of the composite, is assumed to be successfully effectuated in other polymeric systems.

Declaration of Competing Interest

The authors declare that they have no known competing financial interests or personal relationships that could have appeared to influence the work reported in this paper.

CRediT authorship contribution statement

Kata Decsov: Formal analysis, Investigation, Writing – original draft, Visualization, Conceptualization. **Viktor Takács:** Investigation, Visualization. **György Marosi:** Writing – review & editing, Supervision. **Katalin Bocz:** Writing – original draft, Supervision, Funding acquisition, Conceptualization.

Acknowledgements

The authors are thankful to Éva Kiserdei and Panna Vass for her help during the electrospinning process. The project no. 2019-1.3.1-KK-2019-00004 has been implemented with the support provided from the National Research, Development and Innovation Fund of Hungary, financed under the 2019-1.3.1-KK funding scheme. The research was funded by the Hungarian Scientific Research Fund, grant number OTKA PD121171 and FK128352. Support of grant BME FIKP-VÍZ by EMMI is kindly acknowledged. K. Bocz is thankful for the János Bolyai Research Scholarship of the Hungarian Academy of Sciences. K. Bocz was supported by the ÚNKP-20-5-BME New National Excellence Program of the Ministry for Innovation and Technology from the source of the National Research, Development and Innovation Fund.

References

[1] T. Iwata, Biodegradable and bio-based polymers: future prospects of eco-friendly plastics, Angewandte Chemie Int. Ed. 54 (2015) 3210–3215 https://doi.org/, doi:10.1002/anie.201410770.
[2] S. Solarski, M. Ferreira, E. Devaux, Characterization of the thermal properties of PLA fibers by modulated differential scanning calorimetry, Polymer (Guildf) 46 (2005) 11187–11192 https://doi.org/, doi:10.1016/j.polymer.2005.10.027.
[3] G. Koronis, A. Silva, M. Fontul, Green composites: a review of adequate materials for automotive applications, Compos. Part B 44 (2013) 120–127 https://doi.org/, doi:10.1016/j.compositesb.2012.07.004.
[4] R.E. Drumright, P.R. Gruber, D.E. Henton, Polylactic acid technology, Adv. Mater. 12 (2000) 1841–1846 https://doi.org/, doi:10.1002/1521-4095(200012)12:23⟨1841::AID-ADMA1841⟩3.0.CO;2-E.
[5] W. Serrano, A. Meléndez, I. Ramos, N.J. Pinto, Poly(lactic acid)/poly(3-hexylthiophene) composite nanofiber fabrication for electronic applications, Polym. Int. 65 (2016) 503–507 https://doi.org/, doi:10.1002/pi.5081.
[6] B.-H. Li, M.-C. Yang, Improvement of thermal and mechanical properties of poly(L-lactic acid) with 4,4-methylene diphenyl diisocyanate, Polym. Adv. Technol. 17 (2006) 439–443 https://doi.org/, doi:10.1002/pat.731.
[7] D. Garlotta, A literature review of poly(lactic acid), J. Polym. Environ. 9 (2002) 63–84 https://doi.org/, doi:10.1023/A:1020200822435.
[8] F. Carrasco, P. Pagès, J. Gámez-Pérez, O.O. Santana, M.L. Maspoch, Processing of poly(lactic acid): characterization of chemical structure, thermal stability and mechanical properties, Polym. Degrad. Stab. 95 (2010) 116–125 https://doi.org/, doi:10.1016/j.polymdegradstab.2009.11.045.
[9] J.Y. Jang, T.K. Jeong, H.J. Oh, J.R. Youn, Y.S. Song, Thermal stability and flammability of coconut fiber reinforced poly(lactic acid) composites, Compos. Part B 43 (2012) 2434–2438 https://doi.org/, doi:10.1016/j.compositesb.2011.11.003.
[10] S. Li, H. Yuan, T. Yu, W. Yuan, J. Ren, Flame-retardancy and anti-dripping effects of intumescent flame retardant incorporating montmorillonite on poly(lactic acid), Polym. Adv. Technol. 20 (2009) 1114–1120 https://doi.org/, doi:10.1002/pat.1372.
[11] S. Bourbigot, M.Le Bras, S. Duquesne, M. Rochery, Recent advances for intumescent polymers, Macromol. Mater. Eng. 289 (2004) 499–511 https://doi.org/, doi:10.1002/mame.200400007.
[12] A.B. Morgan, J.W. Gilman, An overview of flame retardancy of polymeric materials: application, technology, and future directions, Fire Mater. 37 (2013) 259–279 https://doi.org/, doi:10.1002/fam.2128.
[13] S. Bourbigot, M.Le Bras, R. Delobel, P. Bréant, J. Trémillon, Fire retardant polymers, 5th European Conference, 1995 Salford.
[14] C. Hu, S. Bourbigot, T. Delaunay, M. Collinet, S. Marcille, G. Fontaine, Synthesis of isosorbide based flame retardants: application for polybutylene succinate, Polym. Degrad. Stab. 164 (2019) 9–17 https://doi.org/, doi:10.1016/j.polymdegradstab.2019.03.016.
[15] F. Xiao, G. Fontaine, S. Bourbigot, Recent developments in fire retardancy of polybutylene succinate, Polym. Degrad. Stab. 183 (2021) 109466 https://doi.org/, doi:10.1016/j.polymdegradstab.2020.109466.
[16] D. Vadas, T. Igricz, J. Sarazin, S. Bourbigot, G. Marosi, K. Bocz, Flame retardancy of microcellular poly(lactic acid) foams prepared by supercritical CO_2-assisted extrusion, Polym. Degrad. Stab. 153 (2018) 100–108 https://doi.org/, doi:10.1016/j.polymdegradstab.2018.04.021.
[17] J. Wang, Q. Ren, W. Zheng, W. Zhai, Improved flame-retardant properties of poly(lactic acid) foams using starch as a natural charring agent, Ind. Eng. Chem. Res. 53 (2014) 1422–1430 https://doi.org/, doi:10.1021/ie403041h.
[18] C. Réti, M. Casetta, S. Duquesne, S. Bourbigot, R. Delobel, Flammability properties of intumescent PLA including starch and lignin, Polym. Adv. Technol. 19 (2008) 628–635 https://doi.org/, doi:10.1002/pat.1130.
[19] X. Shi, Y. Ju, M. Zhang, X. Wang, The intumescent flame-retardant biocomposites of poly(lactic acid) containing surface-coated ammonium polyphosphate and distiller's dried grains with solubles (DDGS), Fire Mater. 42 (2018) 190–197 https://doi.org/, doi:10.1002/fam.2479.
[20] X. Wang, Y. Hu, L. Song, S. Xuan, W. Xing, Z. Bai, H. Lu, Flame retardancy and thermal degradation of intumescent flame retardant poly(lactic acid)/starch biocomposites, Ind. Eng. Chem. Res. 50 (2011) 713–720 https://doi.org/, doi:10.1021/ie1017157.
[21] Y. Ju, F. Liao, X. Dai, Y. Cao, J. Li, X. Wang, Flame-retarded biocomposites of poly(lactic acid), distiller's dried grains with solubles and resorcinol di(phenyl phosphate), Compos. Part A 81 (2016) 52–60 https://doi.org/, doi:10.1016/j.compositesa.2015.10.039.
[22] H. Wang, B. Li, Synergistic effects of β-cyclodextrin containing silicone oligomer on intumescent flame retardant polypropylene system, Polym. Adv. Technol. 21 (2010) 691–697 https://doi.org/, doi:10.1002/pat.1484.
[23] G. Crini, S. Fourmentin, É. Fenyvesi, G. Torri, M. Fourmentin, N. Morin-Crini, Cyclodextrins, from molecules to applications, Environ. Chem. Lett. 16 (2018) 1361–1375 https://doi.org/, doi:10.1007/s10311-018-0763-2.
[24] L. Szente, É. Fenyvesi, Cyclodextrin-enabled polymer composites for packaging, Molecules (2018) 23 https://doi.org/, doi:10.3390/molecules23071556.
[25] Z. Aytac, T. Uyar, Core-shell nanofibers of curcumin/cyclodextrin inclusion complex and polylactic acid: enhanced water solubility and slow release of curcumin, Int. J. Pharm. 518 (2017) 177–184 https://doi.org/, doi:10.1016/j.ijpharm.2016.12.061.
[26] P. Wen, D.-H. Zhu, K. Feng, F.-J. Liu, W.-Y. Lou, N. Li, M.-H. Zong, H. Wu, Fabrication of electrospun polylactic acid nanofilm incorporating cinnamon essential oil/β-cyclodextrin inclusion complex for antimicrobial packaging, Food Chem. 196 (2016) 996–1004 https://doi.org/, doi:10.1016/j.foodchem.2015.10.043.
[27] G.M. Estrada, Incorporation of fluoroquinolone/beta cyclodextrin inclusion complex from polylactic acid electrospun fibers and modeling of the release behavior, Revista Mexicana de Ingeniería Química 18 (2019) 737–747 https://doi.org/, doi:10.24275/uam/izt/dcbi/revmexingquim/2019v18n2/Estrada.
[28] Y. Liu, X. Liang, R. Zhang, W. Lan, W. Qin, Fabrication of electrospun polylactic acid/Cinnamaldehyde/β-cyclodextrin fibers as an antimicrobial wound dressing, Polymers (Basel) 9 (2017) 464 https://doi.org/, doi:10.3390/polym9100464.
[29] X. Shan, K. Jiang, J. Li, Y. Song, J. Han, Y. Hu, Preparation of β-cyclodextrin inclusion complex and its application as an intumescent flame retardant for epoxy, Polymers (Basel) 11 (2019) 71 https://doi.org/, doi:10.3390/polym11010071.
[30] X. Zhao, D. Xiao, J.P. Alonso, D.-Y. Wang, Inclusion complex between beta-cyclodextrin and phenylphosphonicdiamide as novel bio-based flame retardant to epoxy: inclusion behavior, characterization and flammability, Mater. Des. 114 (2017) 623–632 https://doi.org/, doi:10.1016/j.matdes.2016.11.093.
[31] L. Zhang, W. Wu, J.H. Li, Z. Wang, L. Wang, S. Chen, New insight into the preparation of flame-retardant thermoplastic polyether ester utilizing β -cyclodextrin as a charring agent, High Perform. Polym. 29 (2017) 422–430 https://doi.org/, doi:10.1177/0954008316648004.
[32] J. Alongi, M. Pošković, A. Frache, F. Trotta, Novel flame retardants containing cyclodextrin nanosponges and phosphorus compounds to enhance EVA combustion properties, Polym. Degrad. Stab. 95 (2010) 2093–2100 https://doi.org/, doi:10.1016/j.polymdegradstab.2010.06.030.
[33] B. Wang, X. Qian, Y. Shi, B. Yu, N. Hong, L. Song, Y. Hu, Cyclodextrin microencapsulated ammonium polyphosphate: preparation and its performance on the thermal, flame retardancy and mechanical properties of ethylene vinyl acetate copolymer, Compos. Part B 69 (2015) 22–30 https://doi.org/, doi:10.1016/j.compositesb.2014.09.015.
[34] L. Huang, M. Gerber, J. Lu, A.E. Tonelli, Formation of a flame retardant-cyclodextrin inclusion compound and its application as a flame retardant for poly(ethylene terephthalate), Polym. Degrad. Stab. 71 (2001) 279–284 https://doi.org/, doi:10.1016/S0141-3910(00)00175-0.
[35] N. Zhang, J. Shen, M.A. Pasquinelli, D. Hinks, A.E. Tonelli, Formation and characterization of an inclusion complex of triphenyl phosphate and β-cyclodextrin and its use as a flame retardant for polyethylene terephthalate, Polym. Degrad. Stab. 120 (2015) 244–250 https://doi.org/, doi:10.1016/j.polymdegradstab.2015.07.014.
[36] W. Wang, Y. Peng, H. Chen, Q. Gao, J. Li, W. Zhang, Surface microencapsulated ammonium polyphosphate with beta-cyclodextrin and its application in wood-flour/polypropylene composites, Polym. Compos. 38 (2017) 2312–2320 https://doi.org/, doi:10.1002/pc.23813.

[37] Z. Zheng, L. Zhang, Y. Liu, H. Wang, A facile and novel modification method of β-cyclodextrin and its application in intumescent flame-retarding polypropylene with melamine phosphate and expandable graphite, J. Polym. Res. 23 (2016) https://doi.org/, doi:10.1007/s10965-015-0905-1.
[38] S. Ding, P. Liu, S. Zhang, C. Gao, F. Wang, Y. Ding, M. Yang, Crosslinking of β-cyclodextrin and combining with ammonium polyphosphate for flame-retardant polypropylene, J. Appl. Polym. Sci. 137 (2020) 48320 https://doi.org/, doi:10.1002/app.48320.
[39] M. Gao, Effect of β-cyclodextrin and ammonium polyphosphate on flame retardancy of jute/polypropylene composites, Mater. Sci. Forum 1001 (2020) 219–223 https://doi.org/, doi:10.4028/www.scientific.net/MSF.1001.219.
[40] Y. Dou, X. Li, T. Zhang, H. Xu, An intumescent flame-retardant layer with β-cyclodextrin as charring agent and its flame retardancy in jute/polypropylene composites, Polym. Bull. (2020) https://doi.org/, doi:10.1007/s00289-020-03315-z.
[41] S.-L. Zeng, C.-Y. Xing, L. Chen, L. Xu, B.-J. Li, S. Zhang, Green flame-retardant flexible polyurethane foam based on cyclodextrin, Polym. Degrad. Stab. 178 (2020) 109171 https://doi.org/, doi:10.1016/j.polymdegradstab.2020.109171.
[42] M.Le Bras, S. Bourbigot, Y.Le Tallec, J. Laureyns, Synergy in intumescence—application to β-cyclodextrin carbonisation agent in intumescent additives for fire retardant polyethylene formulations, Polym. Degrad. Stab. 56 (1997) 11–21 https://doi.org/, doi:10.1016/S0141-3910(96)00190-5.
[43] Q. Li, J. Wang, L. Chen, H. Shi, J. Hao, Ammonium polyphosphate modified with β-cyclodextrin crosslinking rigid polyurethane foam: enhancing thermal stability and suppressing flame spread, Polym. Degrad. Stab. 161 (2019) 166–174 https://doi.org/, doi:10.1016/j.polymdegradstab.2019.01.024.
[44] J.-X. Feng, S.-P. Su, J. Zhu, An intumescent flame retardant system using β-cyclodextrin as a carbon source in polylactic acid (PLA), Polym. Adv. Technol. 22 (2011) 1115–1122 https://doi.org/, doi:10.1002/pat.1954.
[45] E.L. Teoh, W.S. Chow, M. Jaafar, β -cyclodextrin as a partial replacement of phosphorus flame retardant for poly(lactic acid)/poly(methyl methacrylate): a more environmental friendly flame-retarded blends, Polym. Plast. Technol. Eng. 56 (2017) 1680–1694 https://doi.org/, doi:10.1080/03602559.2017.1289396.
[46] H. Vahabi, M. Shabanian, F. Aryanasab, F. Laoutid, S. Benali, M.R. Saeb, F. Seidi, B.K. Kandola, Three in one: β -cyclodextrin, nanohydroxyapatite, and a nitrogen-rich polymer integrated into a new flame retardant for poly (lactic acid), Fire Mater. 42 (2018) 593–602 https://doi.org/, doi:10.1002/fam.2513.
[47] Y. Zhang, P. Han, Z. Fang, Synthesis of phospholipidated β-cyclodextrin and its application for flame-retardant poly(lactic acid) with ammonium polyphosphate, J. Appl. Polym. Sci. 135 (2018) 46054 https://doi.org/, doi:10.1002/app.46054.
[48] K. Bocz, T. Krain, G. Marosi, Effect of particle size of additives on the flammability and mechanical properties of intumescent flame retarded polypropylene compounds, Int. J. Polym. Sci. 2015 (2015) 1–7 https://doi.org/, doi:10.1155/2015/493710.
[49] H. Vahabi, H. Wu, M.R. Saeb, J.H. Koo, S. Ramakrishna, Electrospinning for developing flame retardant polymer materials: current status and future perspectives, Polymer (Guildf) 217 (2021) 123466 https://doi.org/, doi:10.1016/j.polymer.2021.123466.
[50] E. Gallo, Z. Fan, B. Schartel, A. Greiner, Electrospun nanofiber mats coating-new route to flame retardancy, Polym. Adv. Technol. 22 (2011) 1205–1210 https://doi.org/, doi:10.1002/pat.1994.
[51] L. Zhang, W. Liu, X. Wen, J. Chen, C. Zhao, M. Castillo-Rodríguez, L. Yang, X.Q. Zhang, R. Wang, D.Y. Wang, Electrospun submicron NiO fibers combined with nanosized carbon black as reinforcement for multi-functional poly(lactic acid) composites, Compos. Part A 129 (2020) 105662 https://doi.org/, doi:10.1016/j.compositesa.2019.105662.
[52] Z.I. Yildiz, A. Celebioglu, T. Uyar, Polymer-free electrospun nanofibers from sulfobutyl ether 7 -beta-cyclodextrin (SBE 7 -β-CD) inclusion complex with sulfisoxazole: fast-dissolving and enhanced water-solubility of sulfisoxazole, Int. J. Pharm. 531 (2017) 550–558 https://doi.org/, doi:10.1016/j.ijpharm.2017.04.047.
[53] P. Vass, Z.K. Nagy, R. Kóczián, C. Fehér, B. Démuth, E. Szabó, S.K. Andersen, T. Vigh, G. Verreck, I. Csontos, G. Marosi, E. Hirsch, Continuous drying of a protein-type drug using scaled-up fiber formation with HP-β-CD matrix resulting in a directly compressible powder for tableting, Eur. J. Pharm. Sci. 141 (2020) 105089 https://doi.org/, doi:10.1016/j.ejps.2019.105089.
[54] P. Vass, B. Démuth, A. Farkas, E. Hirsch, E. Szabó, B. Nagy, S.K. Andersen, T. Vigh, G. Verreck, I. Csontos, G. Marosi, Z.K. Nagy, Continuous alternative to freeze drying: manufacturing of cyclodextrin-based reconstitution powder from aqueous solution using scaled-up electrospinning, J. Control. Release 298 (2019) 120–127 https://doi.org/, doi:10.1016/j.jconrel.2019.02.019.
[55] H. Vahabi, B.K. Kandola, M.R. Saeb, Flame Retardancy Index for thermoplastic composites, Polymers (Basel) 11 (2019) 1–10 https://doi.org/, doi:10.3390/polym11030407.
[56] K. Bocz, T. Igricz, M. Domonkos, T. Bárány, G. Marosi, Self-extinguishing polypropylene with a mass fraction of 9% intumescent additive II – influence of highly oriented fibres, Polym. Degrad. Stab. 98 (2013) 2445–2451 https://doi.org/, doi:10.1016/j.polymdegradstab.2013.06.011.
[57] F. Trotta, M. Zanetti, G. Camino, Thermal degradation of cyclodextrins, Polym. Degrad. Stab. 69 (2000) 373–379 https://doi.org/, doi:10.1016/S0141-3910(00)00084-7.
[58] W. Yin, L. Chen, F. Lu, P. Song, J. Dai, L. Meng, Mechanically Robust, Flame-retardant poly(lactic acid) biocomposites via combining cellulose nanofibers and ammonium polyphosphate, ACS Omega 3 (2018) 5615–5626 https://doi.org/, doi:10.1021/acsomega.8b00540.
[59] K. Decsov, K. Bocz, B. Szolnoki, S. Bourbigot, G. Fontaine, D. Vadas, G. Marosi, Development of bioepoxy resin microencapsulated ammonium-polyphosphate for flame retardancy of polylactic acid, Molecules 24 (2019) 4123 https://doi.org/, doi:10.3390/molecules24224123.